

Shahinoor Alam^{1*}, Mohammad Asaduzzaman Chowdhury¹

¹Dhaka University of Engineering and Technology, Department of Mechanical Engineering, Gazipur, Gazipur-1707, Bangladesh

*Corresponding author. majshahin4282@gmail.com

Received (Otrzymano) 9.03.2020

MICROMECHANICAL ANALYSIS OF GLASS FIBER REINFORCED EPOXY COMPOSITES AND CASE STUDY OF MACRO-MECHANICAL OBSERVATION

This paper was written and formulated based on the micromechanical analysis of unidirectional glass fiber reinforced epoxy composite lamina. To simplify the calculations and achieve acceptable results, a few assumptions like idealized packing, the representative volume element (RVE), uniform strain boundary condition, statistically homogeneous unidirectional fiber reinforced composites, etc. are taken into consideration. Translational symmetric transformation was applied and established mathematical models are presented to obtain the values of the effective material properties by means of the simple strength of materials approach so that they can be compared with the semi-empirical model. In addition, a parametric study was carried out to verify the dependency of the fiber and matrix on the overall effective material properties. This will ultimately help to develop the required glass fiber reinforced epoxy composites for their specific applications.

Keywords: micromechanical analysis, effective material properties, fiber glass, epoxy composite, RVE

INTRODUCTION

A composite (or composition) material refers to a material that is produced from at least two constituents with a combination of considerably distinct chemical or physical properties. These properties eventually create a material whose characteristics are radically different from its individual elements. These individual components continue to be separated from the finished material, which helps to distinguish composites from solid solutions and/or mixtures [1]. Composite materials can be fabricated to attain desired properties by correctly selecting their components, their proportions, their distributions, their morphologies, their degrees of crystallinity, their crystallographic textures, as well as the structure and composition of the interface between the components [2]. Because of their strong compositional ability, composites can be used for different applications like the automobile, aerospace, watercraft construction, electronics, energy, biomedical and other industries [3]. Composites are being used by more industrialists due to their high strength to weight ratio and stiffness to weight ratio [4]. There are four types of composites: fibrous, laminated, particulate, and hybrid. Fiber reinforced composites usually consist of two phases: one is the matrix and the other is fiber. However, most of the existing research on glass fiber reinforced epoxy composites suggests that many factors have a strong impact on their mechanical and physical properties; they include the various kinds of glass fibers and fillers, the aspect ratio, weight/volume fraction, the

various moduli and strengths, matrix types and strengths, bonding of the interface between the matrix and fiber for the purpose of enabling stress transfer, among others [5].

Micromechanical analysis is an important method to understand the mechanical behavior of composite materials with complicated and sophisticated microstructures like fiber or particulate reinforced composites, textile composites, etc. [6]. The mechanical or physical properties of composites depend on the microstructure, which is designed during its manufacturing process [7]. The mass fraction and volume fraction of the reinforcing material must be known before its processing. Ultimately, the design of the composite is limited to some extent, which results in complex and micromechanical interaction. This creates a dilemma in modeling the relation between the microstructure and the characteristics of the material. However, to simplify the calculations and bring about acceptable results, a few assumptions (like idealized packing, the representative volume element, uniform strain boundary condition, statistically homogeneous unidirectional fiber reinforced composites, etc.) are taken into consideration. This also helps to simplify the finite element model to some extent [8, 9].

A statistically homogeneous material means that the local material properties are constant when they are averaged over a representative volume element. Furthermore, it is possible to replace the real disordered

material by a homogeneous one in which the local material properties are averaged over the representative volume element in the real material [10]. To make effective use of unidirectional glass fiber reinforced composite materials, knowing about their properties and performances when subjected to loads is essential. Many aspects of their behavior are directly associated with the microscopic structure of these materials. The desire to understand these materials drives the research in this field into the micromechanics of this type of materials [11]. Against this background, the objective of this work is to carry out micromechanical analysis of statistically homogeneous unidirectional glass fiber reinforced epoxy composite lamina to develop the required glass fiber reinforced epoxy composites with the intended properties for their specific application.

MICROMECHANICAL ANALYSIS AND COMPUTATIONAL METHODS

The micromechanics of lamina help the designer to select the constituents of a composite material to compose the laminated structure. The lamina is simply looked at as a material whose properties are different in various directions, but not different from one location to another.

For micromechanical analysis, a nonhomogeneous lamina with fibers and a matrix is considered as a homogeneous lamina. A unidirectional lamina is not homogeneous, however, it can be assumed that the lamina is homogeneous by focusing on the average response of the lamina to mechanical and hygrothermal loads (Fig. 1).

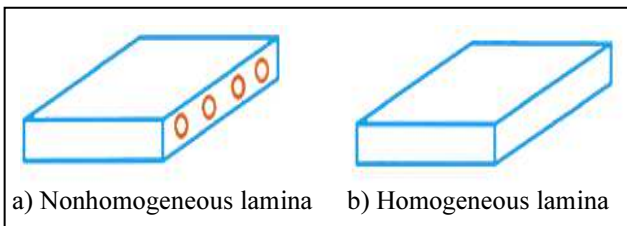


Fig. 1. Nonhomogeneous lamina with fibers and matrix (a) compared to homogeneous lamina (b)

The basis of calculating the fiber content of a composite is very important. It is given in terms of mass or volume. Volume and mass fractions are not equal and the mismatch between mass and volume fractions increases as the ratio between the density of fiber and matrix differs from one another. Considering a composite consisting of glass fiber (E-glass or S-glass) and an epoxy matrix and taking the required symbol notations ($v_{c,f,m}$ - volume of composite, glass fiber, and matrix respectively; $\rho_{c,f,m}$ - density of composite, glass fiber, and matrix respectively; $\omega_{c,f,m}$ - mass of composite, fiber, and matrix respectively) the already established required mathematical formulae can be used as follows:

For volume fractions:

$$V_f = \frac{v_f}{v_c} \quad (1)$$

$$V_m = \frac{v_m}{v_c} \quad (2)$$

$$V_f + V_m = 1 \quad (3)$$

$$v_f + v_m = v_c \quad (4)$$

where: V_f - volume fraction of fiber in the composite lamina; V_m - volume fraction of epoxy matrix in the composite lamina.

For mass fractions:

$$W_f = \frac{\omega_f}{\omega_c} \quad (5)$$

$$W_m = \frac{\omega_m}{\omega_c} \quad (6)$$

$$W_f + W_m = 1 \quad (7)$$

$$\omega_f + \omega_m = \omega_c \quad (8)$$

$$W_f = \frac{\rho_f}{\rho_c} V_f \quad (9)$$

$$W_m = \frac{\rho_m}{\rho_c} V_m \quad (10)$$

where: W_f - mass fraction of fiber in the composite lamina; W_m - mass fraction of epoxy matrix in the composite lamina.

For density:

$$\omega_c = \omega_f + \omega_m \quad (11)$$

$$\rho_c = \rho_f v_f + \rho_m v_m \quad (12)$$

$$v_c = v_f + v_m \quad (13)$$

$$\frac{1}{\rho_c} = \frac{W_f}{\rho_f} + \frac{W_m}{\rho_m} \quad (14)$$

For void content

Voids cause the theoretical density of the composite to be higher than the actual density and are detrimental to its mechanical properties. A decrease of 2 to 10 percent in the preceding matrix-dominated properties generally take place with every 1% increase in the void content [12]. For composites with a certain volume of voids v_v , the volume fraction of voids V_v is defined as:

$$V_v = \frac{v_v}{v_c} \quad (15)$$

$$v_c = v_f + v_m + v_v \quad (16)$$

$$v_c = \frac{\omega_c}{\rho_{ce}} \quad (17)$$

$$v_f + v_m = \frac{\omega_c}{\rho_{ct}} \quad (18)$$

$$\frac{\omega_c}{\rho_{ce}} = \frac{\omega_c}{\rho_{ct}} + v_v \quad (19)$$

$$V_v = \frac{\omega_c}{\rho_{ce}} \left(\frac{\rho_{ct} - \rho_{ce}}{\rho_{ct}} \right) \quad (20)$$

$$V_v = \frac{v_v}{v_c} = \frac{\rho_{ct} - \rho_{ce}}{\rho_{ct}} \quad (21)$$

where: ρ_{ce} - experimental density of composite lamina;
 ρ_{ct} - theoretical density of composite lamina.

TYPICAL PROPERTIES OF GLASS FIBER AND EPOXY MATRIX

Glass fiber has now emerged as the most popular form of reinforcement fiber when it comes to composite construction, making up more than 90% of global consumption. This is mainly attributed to its durable strength, smooth processing and affordability. There are different types of glass fiber available for practical use. The main types are E-glass and S-glass. The ‘E’ in E-glass stands for electrical because it is designed for electrical applications. However, it is used for many other purposes now such as decorations and structural applications. S-glass, having a higher content of silica, retains its strength at higher temperatures compared to E-glass and has a higher fatigue strength. It is used mainly for aerospace applications. Some property differences are given in Table 1.

TABLE 1. Typical properties of glass fibers and epoxy matrix

Properties	Units	Glass Fiber		Epoxy
		E-glass	S-glass	
Axial modulus	[GPa]	72.40	85.00	3.40
Transverse modulus	[GPa]	72.40	85.00	3.40
Shear modulus	[GPa]	30.00	35.42	1.31
Poisson's ratio	[-]	0.22	0.20	0.30
Axial coefficient of thermal expansion	[$\mu\text{m}/\text{m}/^\circ\text{C}$]	5.04	5.00	63.00
Transverse coefficient of thermal expansion	[$\mu\text{m}/\text{m}/^\circ\text{C}$]	5.04	5.00	63.00
Axial tensile strength	[MPa]	1950	1550	72
Transverse tensile strength	[MPa]	1950	1550	72
Shear strength	[MPa]	30.00	35.00	34.00
Specific gravity	[-]	2.54	2.50	1.20

The difference in the properties is due to the compositions of E-glass and S-glass fibers. The main elements in the two types of fibers are given in Table 2.

TABLE 2. Chemical composition of E-glass and S-glass fibers

Material	[% Weight]	
	E-glass	S-glass
Silicon oxide	54	64
Aluminum oxide	15	25
Calcium oxide	17	0.01
Magnesium oxide	4.5	10
Boron oxide	8	0.01
Others	1.5	0.8

With regard to plastics reinforced with fiber, epoxy is generally used as the matrix that effectively binds the fibers [13]. One of the greatest advantages of epoxy is its compatibility with nearly all reinforcing fibers such as carbon fiber, glass fiber, basalt, and aramid.

EVALUATION OF ELASTIC MODULI BY STRENGTH OF MATERIALS APPROACH

The modeling of fiber reinforced composites begins with establishing the smallest volume in which a measurement can be made that will yield a volume representative of the whole [14]. From a unidirectional lamina, a representative volume element (RVE) as per Figure 2 is considered, and the following assumptions are made in the strength of materials approach model:

- The bond between the fibers and matrix is perfect.
- The elastic moduli, diameters, and space between the fibers are uniform.
- The fibers are continuous and parallel.
- The fibers and matrix follow Hooke’s law (linearly elastic).
- The fibers possess uniform strength.
- The composite is free of voids.

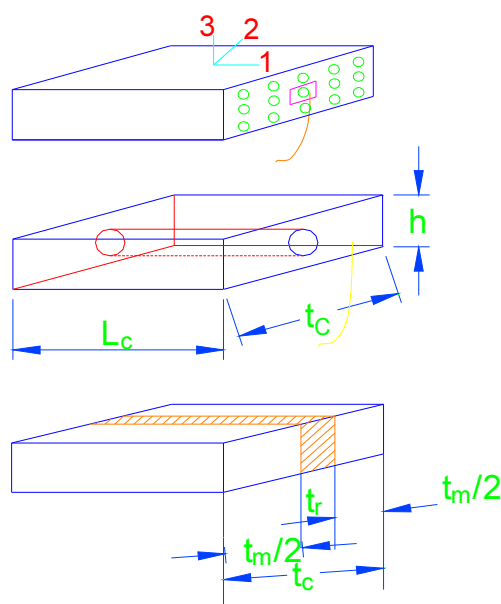


Fig. 2. Representative volume element of unidirectional lamina

Longitudinal Young’s modulus

Assuming in Figure 3 that the fibers, matrix, and composite follow Hooke’s law and that the fibers and the matrix are isotropic, the longitudinal Young’s modulus as a weighted mean of the fiber and matrix modulus can be expressed as:

$$E_1 = E_f V_f + E_m V_m \quad (22)$$

The ratio of the load taken by the fibers F_f to the load taken by the composite F_c is a measure of the load shared by the fibers and can be expressed as:

$$\frac{F_f}{F_c} = \frac{E_f}{E_1} V_f \tag{23}$$

where $E_{1,f,m}$ - elastic moduli of the composite, fiber, and matrix, respectively.

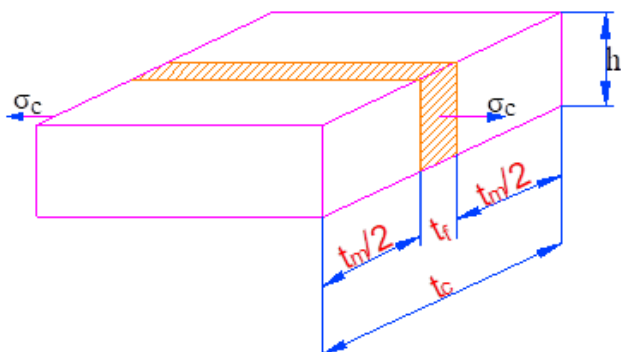


Fig. 3. Longitudinal stress applied to representative volume element to calculate longitudinal Young's modulus for unidirectional lamina

The analytical values from equation (22) and equation 23 of the longitudinal Young's modulus and the ratio of the load taken by the fibers (E-glass and S-glass) to the load taken by the composite are determined as in Table 3.

TABLE 3. Fraction of load of composite carried by fibers as function of fiber volume fraction for constant fiber to matrix moduli ratio and longitudinal Young's moduli of composites

Volume fraction of glass fiber (V_f)	Volume fraction of matrix (V_m)	Fiber to matrix moduli ratio, E_f/E_m		Longitudinal Young's modulus of composite, E_1 [GPa]		Fiber to composite load ratio, F_f/F_c	
		E-glass	S-glass	E-glass	S-glass	E-glass	S-glass
0.1	0.9	21.30	25.00	10.30	11.56	0.703	0.735
0.2	0.8	21.30	25.00	17.20	19.72	0.842	0.862
0.3	0.7	21.30	25.00	24.10	27.88	0.901	0.915
0.4	0.6	21.30	25.00	31.00	36.04	0.934	0.943
0.5	0.5	21.30	25.00	37.90	44.20	0.955	0.962
0.6	0.4	21.30	25.00	44.80	52.36	0.970	0.974
0.7	0.3	21.30	25.00	51.70	60.52	0.980	0.983
0.8	0.2	21.30	25.00	58.60	68.68	0.988	0.990
0.9	0.1	21.30	25.00	65.50	76.84	0.995	0.996

Transverse Young's modulus

Assuming that the composite is stressed in the transverse direction as in Figure 4, the transverse Young's modulus of a glass fiber/epoxy lamina with a fiber and matrix volume fraction can be expressed as:

$$\frac{1}{E_2} = \frac{V_f}{E_f} + \frac{V_m}{E_m} \tag{24}$$

where E_2 - transverse Young's modulus of a glass/epoxy lamina.

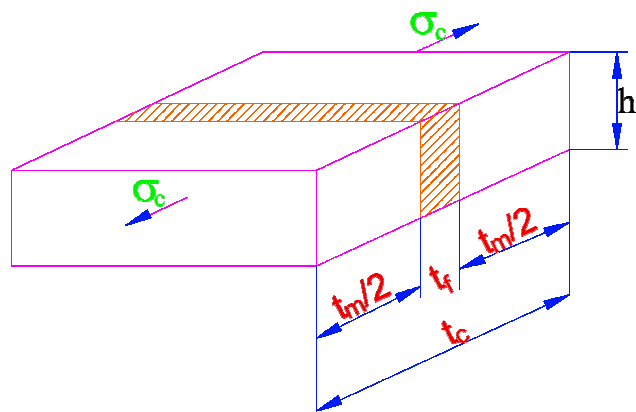


Fig. 4. Transverse stress applied to representative volume element to calculate transverse Young's modulus of unidirectional lamina

The analytical values of the transverse Young's modulus of the composite are determined from equation (24) and compared with the Young's modulus of the matrix (Table 4).

TABLE 4. Transverse Young's modulus as function of fiber volume fraction

Volume fraction of glass fiber (V_f)	Volume fraction of matrix (V_m)	Transverse Young's modulus of composite, E_2 [GPa]		Composite to matrix transverse Young's modulus ratio (E_2/E_m)	
		E-glass	S-glass	E-glass	S-glass
0.1	0.9	3.75	3.76	1.105	1.106
0.2	0.8	4.20	4.21	1.235	1.238
0.3	0.7	4.76	4.78	1.400	1.406
0.4	0.6	5.50	5.52	1.616	1.624
0.5	0.5	6.50	6.54	1.910	1.924
0.6	0.4	7.94	8.02	2.336	2.359
0.7	0.3	10.21	10.37	3.004	3.050
0.8	0.2	14.31	14.66	4.209	4.312
0.9	0.1	23.80	25.00	7.000	7.353

In-plane shear modulus

Applying pure shear stress τ_c to a lamina and assuming the shear stresses in the fiber, matrix and composite are equal as in Figure 5, the shear moduli of the composite may be expressed as:

$$G_f = \frac{E_f}{2(1+V_f)} \tag{25}$$

$$G_m = \frac{E_m}{2(1+V_m)} \tag{26}$$

$$\frac{1}{G_{12}} = \frac{V_f}{G_f} + \frac{V_m}{G_m} \tag{27}$$

where $G_{12,f,m}$ - shear moduli of the composite, fiber, and matrix, respectively.

The analytical values of the in-plane shear modulus of the unidirectional lamina is determined with equations (25)-(27) as shown in Table 5.

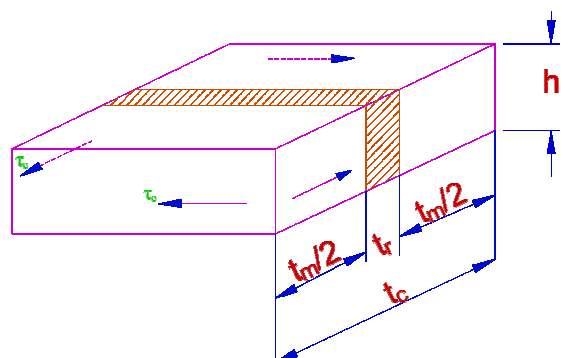


Fig. 5. In-plane shear stress applied to representative volume element to find in-plane shear modulus of unidirectional lamina

TABLE 5. Analytical values of in-plane shear modulus of unidirectional glass fiber/epoxy lamina

Volume fraction of glass fiber (V_f)	Volume fraction of matrix (V_m)	In-plane shear modulus of glass fiber, G_f [GPa]		In-plane shear modulus of matrix, G_m [GPa]	In-plane shear modulus of unidirectional lamina G_{12} [GPa]	
		E-glass	S-glass		E-glass	S-glass
0.1	0.9	32.91	38.64	0.895	0.991	0.992
0.2	0.8	30.17	35.42	0.944	1.232	1.172
0.3	0.7	27.85	32.69	1.000	1.407	1.410
0.4	0.6	25.86	30.36	1.062	1.723	1.729
0.5	0.5	24.13	28.33	1.136	2.170	2.184
0.6	0.4	22.63	26.56	1.214	2.809	2.840
0.7	0.3	21.29	25.00	1.308	3.813	3.886
0.8	0.2	20.11	23.61	1.417	5.527	5.713
0.9	0.1	19.05	22.37	1.545	8.932	9.528

COEFFICIENT OF THERMAL EXPANSION

When a body undergoes a temperature change, its dimensions relative to its original dimensions change in proportion to the temperature change. The coefficient of thermal expansion is defined as the change in the linear dimension of a body per unit length per unit change of temperature.

TABLE 6. Longitudinal and transverse coefficients of thermal expansion as function of fiber volume fraction for glass fiber/epoxy unidirectional lamina

Sl	Fiber volume fraction (V_f)	Longitudinal Young's modulus of composite, E_1 [GPa]		Transverse Young's modulus of composite, E_2 [GPa]		Longitudinal coefficients of thermal expansion, α_1 [$\mu\text{m}/\text{m}/^\circ\text{C}$]		Transverse coefficients of thermal expansion, α_2 [$\mu\text{m}/\text{m}/^\circ\text{C}$]	
		E-glass	S-glass	E-glass	S-glass	E-glass	S-glass	E-glass	S-glass
1.	0.0					63.00	63.00	63.00	63.00
2.	0.1	10.30	11.56	3.75	3.76	22.26	20.35	67.82	68.41
3.	0.2	17.20	19.72	4.20	4.21	14.21	13.00	62.71	63.08
4.	0.3	24.10	27.88	4.76	4.78	10.76	9.95	56.20	56.44
5.	0.4	31.00	36.04	5.50	5.52	8.85	8.28	49.22	49.39
6.	0.5	37.90	44.20	6.50	6.54	7.64	7.23	42.04	42.14
7.	0.6	44.80	52.36	7.94	8.02	6.80	6.51	34.74	34.80
8.	0.7	51.70	60.52	10.21	10.37	6.18	5.98	27.37	27.39
9.	0.8	58.60	68.68	14.31	14.66	5.71	5.57	20.30	19.95
10.	0.9	65.50	76.84	23.80	25.00	5.34	5.26	12.51	12.49

For a unidirectional lamina, the dimension changes differ in two directions (1 and 2). Thus, the two coefficients of thermal expansion are defined as:

α_1 - linear coefficient of thermal expansion in direction 1, $\text{m}/\text{m}/^\circ\text{C}$ ($\text{in.}/\text{in.}/^\circ\text{F}$)

α_2 - linear coefficient of thermal expansion in direction 2, $\text{m}/\text{m}/^\circ\text{C}$ ($\text{in.}/\text{in.}/^\circ\text{F}$)

The following are the expressions developed for the two thermal expansion coefficients using the thermo-elastic extreme principle.

$$\alpha_1 = \frac{1}{E_1} (\alpha_f E_f V_f + \alpha_m E_m V_m) \tag{28}$$

$$\alpha_2 = (1 + \nu_f) \alpha_f V_f + (1 + \nu_m) \alpha_m V_m - \alpha_1 \nu_{12} \tag{29}$$

where α_f and α_m - coefficients of thermal expansion for the fiber and the matrix respectively;

and ν_{12} = major Poisson's ratio = $\nu_f V_f + \nu_m V_m$

where, ν_f = Poisson's ratio of fiber and ν_m = Poisson's ratio of the matrix.

By applying equations (28) and (29), the analytical values of the longitudinal and transverse coefficient of thermal expansion as a function of the fiber volume fraction of glass fiber/epoxy lamina is determined (Table 6).

SEMI-EMPIRICAL MODELS

The values obtained for the transverse Young's modulus and in-plane shear modulus by means of equations (24) and (27), respectively, do not conform well with the experimental results shown in Tables 6 and 7. This indicates the need for better modeling techniques [15]. Unfortunately, they are available only in complicated equations or graphical forms. To overcome these constraints, Halpin and Tsai developed a semi-empirical model for design purposes, which can be used over a wide range of elastic properties and fiber volume fractions [2]. They are simple equations for best curve fitting to results that are based on elasticity, and the parameters used in the curve have their own standard meaning.

Longitudinal Young’s modulus (by Halpin-Tsai)

The Halpin-Tsai equation for the longitudinal Young’s modulus (E_1) is the same as that obtained by the strength of materials approach.

Transverse Young’s modulus (by Halpin-Tsai)

The transverse Young’s modulus (Fig. 6), E_2 is given by:

$$\frac{E_2}{E_m} = \frac{1+\xi\eta V_f}{1-\eta V_f} \tag{30}$$

$$\eta = \frac{(E_f/E_m)-1}{(E_f/E_m)+\xi} \tag{31}$$

where ξ - the reinforcing factor.

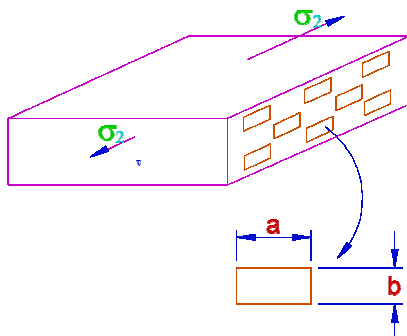


Fig. 6. Concept of direction of loading to calculate transverse Young’s modulus using Halpin-Tsai equations

Using experimental data, the Halpin-Tsai equation is developed for the transverse modulus as a best fit curve and its values are compared with the data of the strength of materials approach (Table 7).

TABLE 7. Theoretical values of transverse Young’s modulus as function of fiber volume fraction and comparison with experimental values for glass fiber/epoxy unidirectional lamina

Sl	Fiber volume fraction V_f	Transverse Young’s modulus, E_2 [GPa]			
		Strength of materials approach		Experimental data	Halpin-Tsai Eq.
		E-glass	S-glass		
1.	0.1	3.75	3.76	10.5	4
2.	0.2	4.20	4.21	13.0	5.2
3.	0.3	4.76	4.78	15.5	6.75
4.	0.4	5.50	5.52	17.0	8.5
5.	0.5	6.50	6.54	14.5	11
6.	0.6	7.94	8.02	19.8	14
7.	0.7	10.21	10.37	12.0	18.5
8.	0.8	14.31	14.66	18.0	26.5
9.	0.9	23.80	25.00	21.0	37.5

In-plane shear modulus (by Halpin-Tsai)

The Halpin-Tsai equations for the in-plane shear modulus, $G_{1,2}$ are

$$\frac{G_{12}}{G_m} = \frac{1+\xi\eta V_f}{1-\eta V_f} \tag{32}$$

$$\eta = \frac{(G_f/G_m)-1}{(G_f/G_m)+\xi} \tag{33}$$

$$\xi = 1 + 40V_f^{10} \tag{34}$$

The value of the reinforcing factor, ξ depends on the fiber geometry, packing geometry, and the loading conditions. For example, for circular fibers in a square array, $\xi = 1$. For a rectangular fiber cross-sectional area of length ‘a’ and width ‘b’ in a hexagonal array, ‘a’ is the direction of loading. The concept of the direction of loading is given in Figure 7.

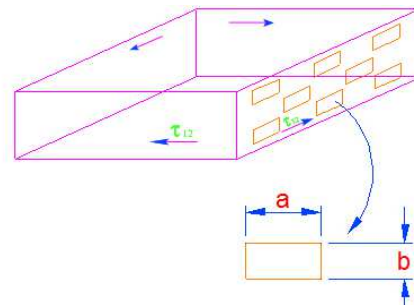


Fig. 7. Concept of direction of loading to calculate in-plane shear modulus using Halpin-Tsai equations

With the help of experimental data, the Halpin-Tsai best fit values (eqs. (32), (33) and (34)) of the in-plane shear modulus of glass fiber/epoxy lamina are determined and compared with the values of the strength of materials approach (Table 8).

TABLE 8. Theoretical values of in-plane shear modulus as function of fiber volume fraction compared with experimental values for glass fiber/epoxy unidirectional lamina

Sl	Fiber volume fraction, V_f	In-plane shear modulus, G_{12} [GPa]			
		Strength of materials approach		Experimental data	Halpin-Tsai Eq.
		E-glass	S-glass		
1.	0.1	0.991	0.992	3.4	1.1
2.	0.2	1.232	1.172	4.4	1.4
3.	0.3	1.407	1.410	4.6	2
4.	0.4	1.723	1.729	4.8	2.9
5.	0.5	2.170	2.184	5.8	4
6.	0.6	2.809	2.840	5.1	5.2
7.	0.7	3.813	3.886	6.0	7
8.	0.8	5.527	5.713	5.8	9.6
9.	0.9	8.932	9.528	6.2	13.6

RESULTS AND DISCUSSION

By changing the volume fraction of the fiber and the matrix and substituting those values in already established mathematical models, the different strengths of the composite materials are tabulated (Table 2) and analyzed. Here the volume fraction varies from 0.1 to 0.9 for both the glass fiber (E-glass and S-glass) and the matrix.

Strength of materials approach

Longitudinal Young's modulus

The ratio of the load carried by the fibers to the load taken by the composite (F_f/F_c) is plotted as a function of the fiber to matrix Young's moduli ratio (E_f/E_m) in Figure 8 for a constant volume of composites but a different volume fraction of glass fiber (V_f) of E-type and S-type glass. It shows that the fiber to matrix moduli ratio does not change as the load taken by the fibers increases.

Figure 9 shows the linear relationship between the longitudinal Young's modulus of a unidirectional lamina and the fiber volume fraction for a typical glass fiber (E-type and S-type glass) epoxy composites.

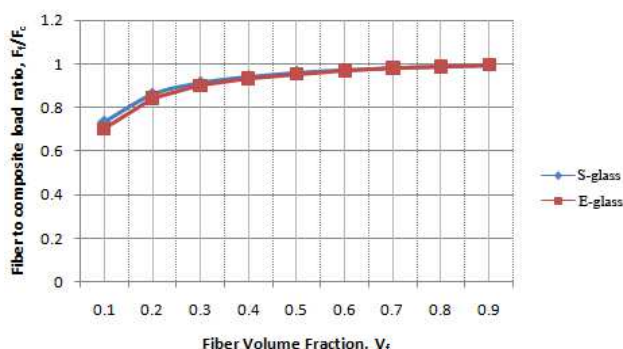


Fig. 8. Ratio of load carried by fibers as function of fiber volume fraction for constant fiber to matrix moduli ratio for typical glass fiber/epoxy lamina

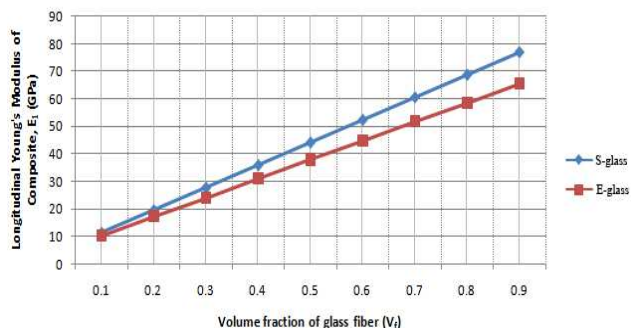


Fig. 9. Longitudinal Young's modulus as function of fiber volume fraction for typical glass fiber/epoxy lamina

Transverse Young's modulus

Figure 10 plots the composite to matrix transverse Young's modulus ratio (E_2/E_m) as a function of the fiber volume fraction for a constant fiber-to-matrix elastic moduli ratio. The transverse Young's modulus of the composite in such cases changes more smoothly as a function of the fiber volume fraction. As the glass fiber (E-type and S-type glass) volume fraction, V_f increases, the transverse Young's modulus ratio, E_2/E_m also increases up to 7.000 and 7.353 for E-glass and S-glass fibers, respectively when V_f is 0.9.

In Figure 11, the transverse Young's modulus is plotted as a function of the fiber volume fraction for a typical glass (E-glass and S-glass) fiber/epoxy lamina. This figure also shows the increasing trend of the

transverse Young's modulus with the increasing glass fiber volume fraction.

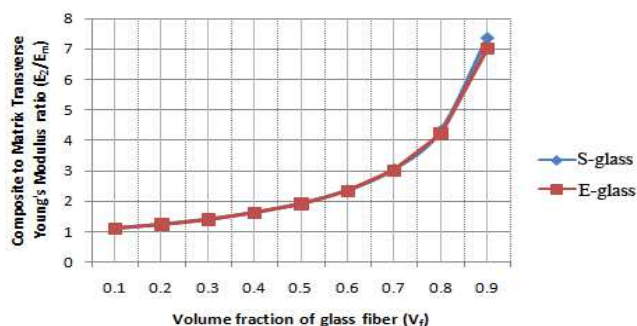


Fig. 10. Composite to matrix transverse Young's modulus ratio as function of fiber volume fraction for glass fiber/epoxy unidirectional lamina

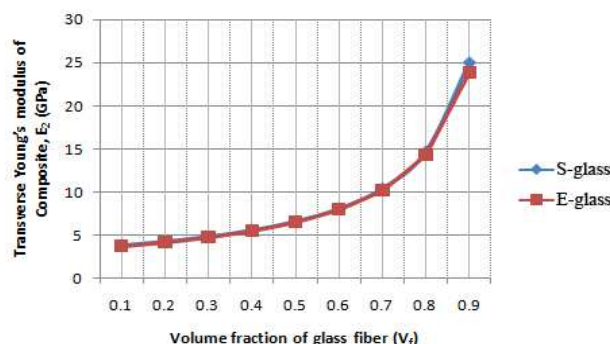


Fig. 11. Transverse Young's modulus of composite as function of fiber volume fraction for glass fiber/epoxy unidirectional lamina

In-plane shear modulus

Figure 12 shows the analytical values of the in-plane shear modulus as a function of the fiber volume fraction for a typical glass fiber/epoxy lamina.

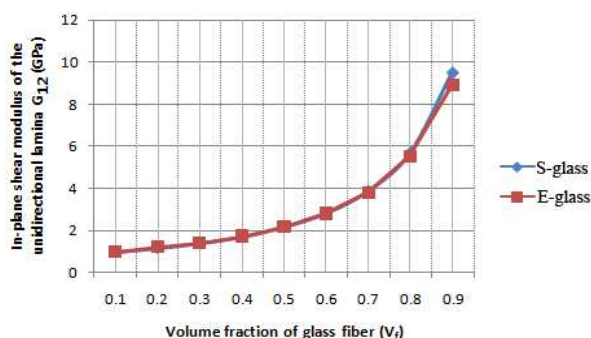


Fig. 12. Theoretical values of in-plane shear modulus as function of fiber volume fraction

For the highest value of V_f , the in-plane shear modulus 8.932 and 9.528 GPa for E-glass and S-glass fibers are obtained when the matrix volume fraction is 0.1.

COEFFICIENT OF THERMAL EXPANSION

Figure 13 shows that the longitudinal coefficient of thermal expansion gradually decreases with an increas-

ing trend of the fiber volume fraction; on the other hand, the transverse coefficient of thermal expansion initially increases and then gradually decreases with an increasing V_f .

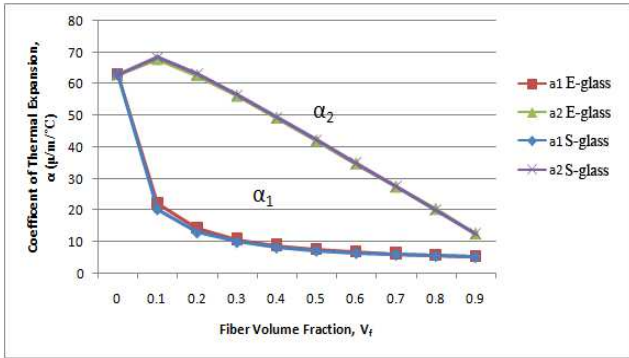


Fig. 13. Longitudinal and transverse coefficients of thermal expansion as function of fiber volume fraction for a glass fiber/epoxy unidirectional lamina

SEMI-EMPIRICAL MODEL (BY HALPIN-TSAI)

Transverse Young's modulus (by Halpin-Tsai)

Figure 14 shows that the values obtained from the best fit curve in comparison to the experimental data and the strength of materials approach data will be the most economical for any design of composite manufacturing.

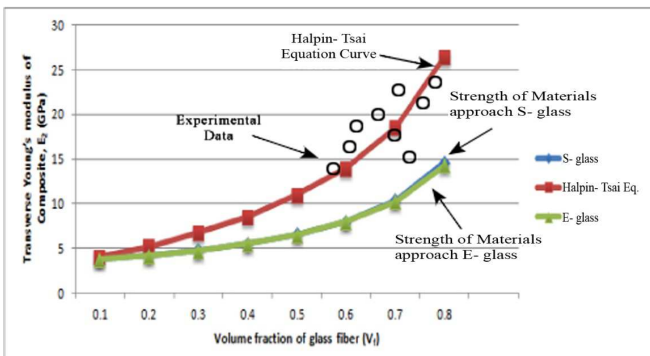


Fig. 14. Theoretical values of transverse Young's modulus as function of fiber Volume fraction and comparison with experimental values for glass fiber/epoxy unidirectional lamina

In-plane shear modulus (by Halpin-Tsai)

The data obtained from the Halpin-Tsai equation for the in-plane shear modulus in comparison with the experimental and strength of materials approach data also shows improved results.

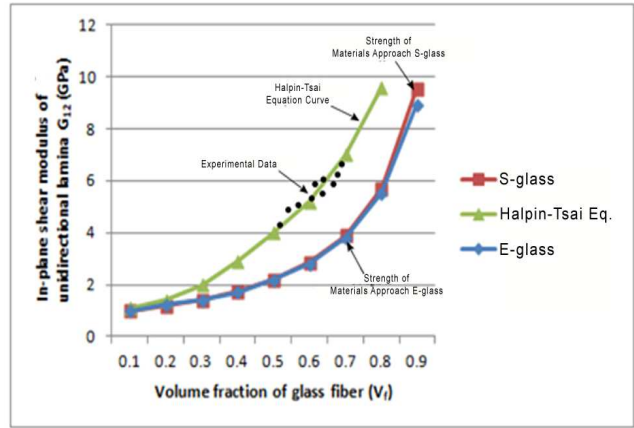


Fig. 15. Theoretical values of in-plane shear modulus as function of fiber volume fraction compared with experimental values for glass fiber/epoxy unidirectional lamina

CASE STUDY: MICRO TO MACRO MECHANICAL ANALYSIS BY MEANS OF EPOXY-BASED GLASS FIBER COMPOSITE FABRICATION

Composite fabrication

Three types of epoxy-based fiber reinforced plastic (FRP) composites that contain varying fillers were produced using the hand lay-up method (Fig. 16). Various percentages (weight related) of epoxy, fibers and fillers were used in the experiments, as depicted in Table 9. In order to obtain the desired level of homogeneity, all the composite samples were prepared in the same way and a similar light compression pressure is applied in all the cases.

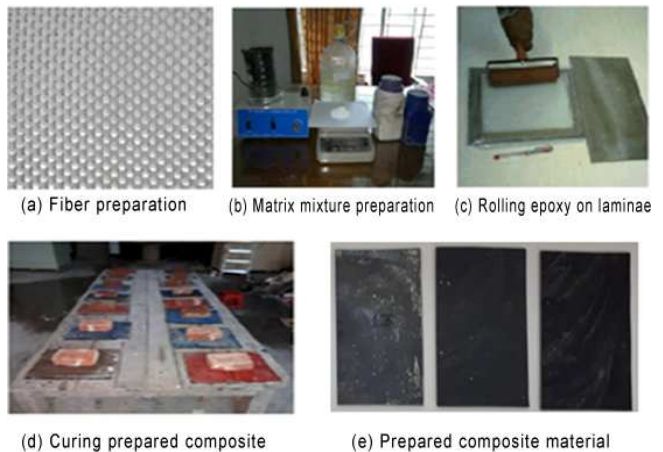


Fig. 16. Fabrication of composite samples

TABLE 9. Composition of FRP [wt.%]

Sample	Fiber stacking sequence	Compositions							
		Matrices [wt.%]		Reinforcement [wt.%]					
		Epoxy (LY556)	Araldite (HY951)	Glass fiber	Filler				Total
		CaCO ₃	Al ₂ O ₃		MgO	CuO			
S1	G/ G/ G/ G/ G	33.33	3.33	58.89	1.11	1.11	1.11	1.11	4.44
S2	G/ G/ G/ G/ G	31.91	3.19	56.38	2.13	2.13	2.13	2.13	8.52
S3	G/ G/ G/ G/ G	30.61	3.06	54.08	3.06	3.06	3.06	3.06	12.24

Tensile strength analysis

Tensile testing was performed by cutting the composite specimen in accordance with the ASTM D638 (ISO 527-2-1B) standard. An M350-10 (Testometric) twin-column range universal testing machine with a speed of 1 mm/min was used within an artificial universal testing range environment for this test. The testing machine is integrated with specialized software/test fixtures that are developed with the specific objective of adhering to globally respected standards. Various weight percentages and blends of filler materials were used to prepare different types of specimens for testing. Both the tensile strain and stress were recorded automatically (Table 10), meanwhile the stress vs strain curves were created.

TABLE 10. Tensile test data

Experiment	Sample composite	Force @ peak [N]	Stress @ peak [N/mm ²]	Force @ yield [N]	Stress @ yield [N/mm ²]	Strain @ yield [%]	Strain @ break [%]	Young's modulus [N/mm ²]
1	Sample - 1	6256.5	113.08	6255.2	113.057	5.181	5.185	2106.13
	Sample - 2	6307.3	133.666	6307.1	133.662	5.048	5.049	2565.205
	Sample - 3	6224.0	141.879	6223.6	141.87	4.884	4.889	2819.752

Tensile strength

The tensile strength of the composite can be augmented by increasing the number of filler particles. The experiment 1 data of the epoxy composites are displayed in Figure 17. The improvement in the tensile strength is attributed to the filler particles, which created good bonding strength among matrix and the fibers.

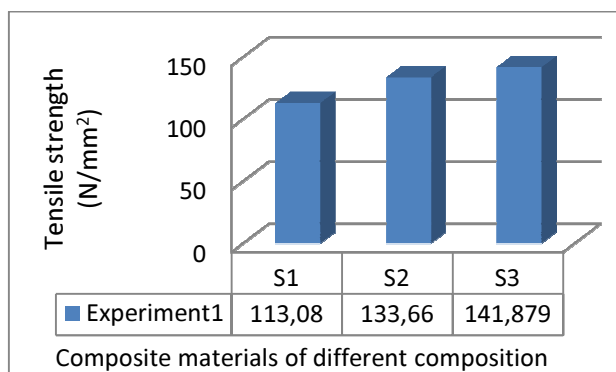


Fig. 17. Tensile strength of different filler particles added epoxy based glass fiber composite

The tendency of an increase in the percentage with regard to tensile strength was observed for all the instances of the prepared composites with CuO. Never-

theless, this increasing trend of tensile strength seems to be lower than the expected percentage. This may be due to inadequate binding and voids at the interfacial level of the composites.

Stiffness

The higher the Young's modulus value, the stiffer the material. Based on comparison of the graphs in Figure 18, it is observed that the FRP Composite S3 with CuO filler sample shows the highest stiffness (2819.752 N/mm²) and can resist deformation well.

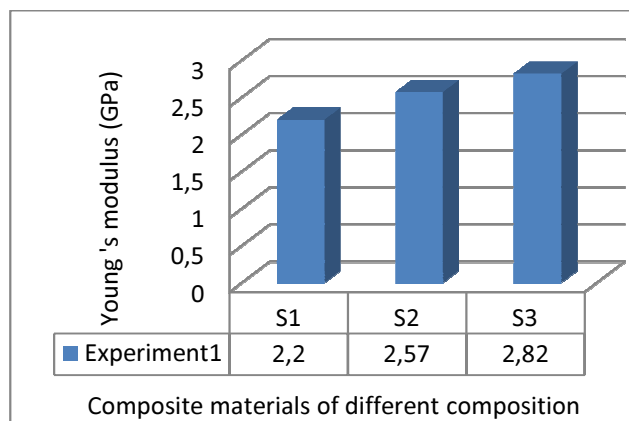


Fig. 18. Comparison of stress vs strain curve of different filler particles added to glass fiber laminated epoxy composites

Thermal gravimetric analysis (TGA)

Thermal Gravimetric Analysis took place between 50 and 1000°C within purging nitrogen, at the heating rate of 5°C min⁻¹ using a TGA Instrument SDT650 Serial No 0650-0180. A sample weighing 25÷45 mg was measured for each round of TG analysis. Plots of the percentage of mass change as a function of time or temperature (TGA curve) and heat flow versus temperature (known as the DSC curve) are the typical results of TGA analysis as shown in Figures 19 to 21. The composite samples (S1, S2 and S3) of Experiment 1 have glass transition temperatures at 75°C, 75°C and 88°C respectively, which are presented in Figures 19, 20 and 21.

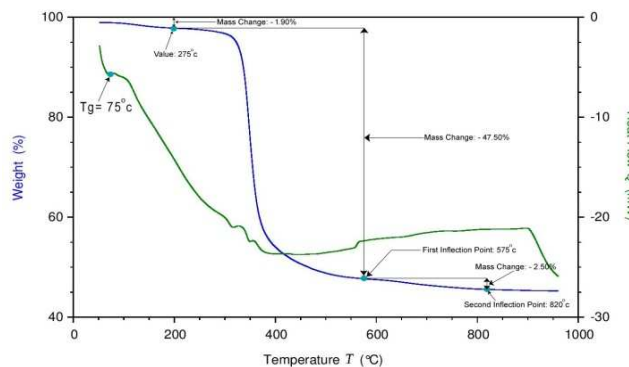


Fig. 19. Composite sample 1 DSC/TGA curves

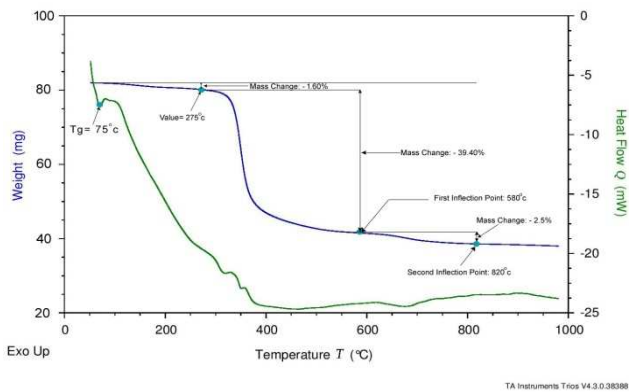


Fig. 20. Composite sample 2 DSC/TGA curves

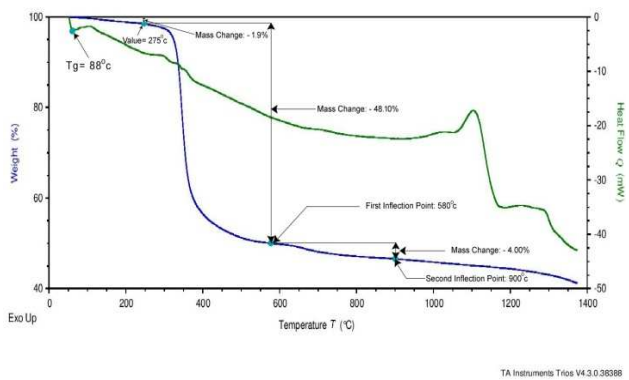


Fig. 21. Composite sample 3 DSC/TGA curves

TABLE 11. TGA results of prepared composites

Sample	Glass transition temperature [°C]	Mass change in percentage 50°C to 275°C	Mass change in percentage 275°C to first inflection	Initial inflection point [°C]	Subsequent inflection point [°C]	Mass change in percentage from both inflection points
S1	75	1.90	47.50	575	820	2.50
S2	75	1.60	39.40	580	820	2.50
S3	88	1.90	48.10	580	900	4.00

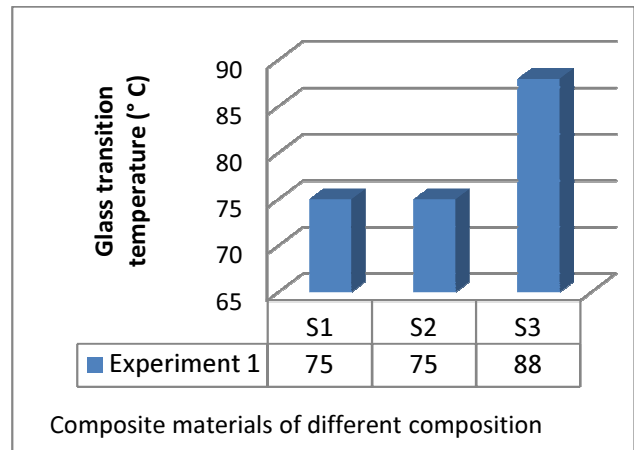


Fig. 22. Trends of glass transition temperature of composite samples

Two factors were considered to take a decision on the areas of fixing the ranges of temperature concerning the changes in mass. Volatility is the first challenge - it includes water as well as residual solvents. According to the findings, 275°C yielded consistent outcomes across all the prepared samples on expected levels (1±2%). The second issue is the inflection point since all the aforementioned samples were found to reflect a gradual alteration of slope within the 580÷590°C range. Employing an initial derivative curve was intended to accurately outline the point of inflection. As depicted in Table 11 and Figure 22, there are differences in the values among the samples lacking proper adhesion at their interfacial level.

SEM (Scanning Electron Microscopy) analysis

The microstructure of the composites was investigated employing SEM (Model: Hitachi SU-1510). The morphological characterization of the composite surface was observed in the aforementioned scanning electron microscope. Significant differences in the internal structure and distribution of fillers in the sample volume of the prepared composites were found. SEM photomicrographs of a cross-sectional layer of the specimens are displayed in Figure 23. From this figure, it is observed that the matrix, fillers and fibers are not well bonded in the S1, S2 and S3 specimens.

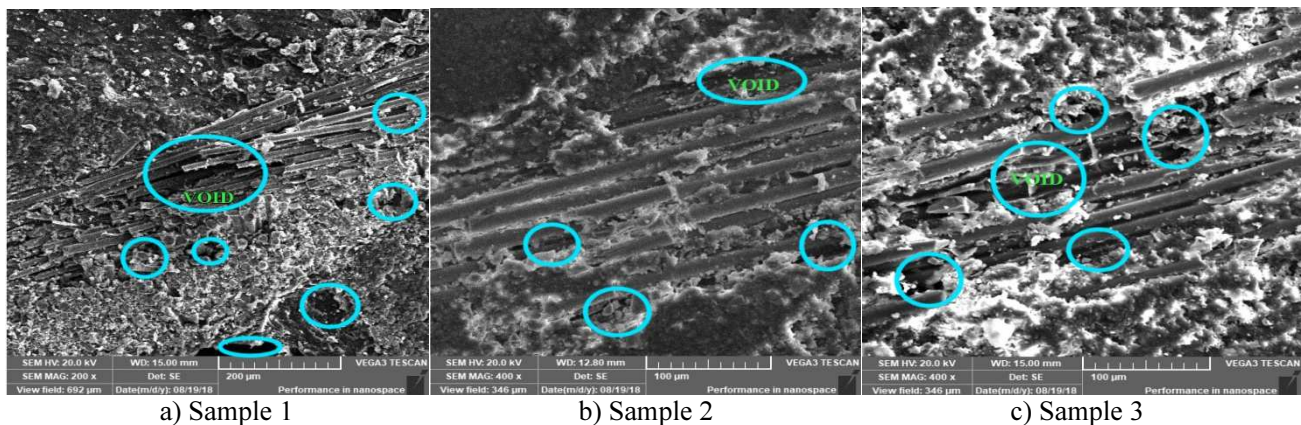


Fig. 23. Cross-sectional SEM micrographs of all composite samples

The lack of adhesion between the glass fiber lamina and the filler materials is evident on the fractured surfaces. This indicates insufficient interaction at the interfacial level and potentially elucidates a decline in the quality of thermal and mechanical attributes. There was a positive correlation between the content and filler interactions. This, in turn, may also explain the deterioration physical traits, given that the stress transference was less efficacious.

CONCLUSIONS

Glass fiber is a widely available material. The uses of such a kind of materials for advanced engineering applications are practically endless owing to their high mechanical properties. The studies of the mechanical properties exhibited by glass fiber are in the advanced stage. Nonetheless, there are still many important unresolved problems. Micromechanical analysis helps to put theoretical values into practical experiments to solve those problems.

In this work, micromechanical analysis of glass fiber (E-type glass and S-type glass) epoxy lamina was carried out by means of different modeling techniques and compared with the best fit model (Halpin-Tsai equation). The analytical results and their comparison show:

- As the load taken by the fiber increased, the fiber to matrix moduli ratio did not change with increasing the fiber volume fraction, but the fiber to matrix ratio of E-glass was less than S-glass fiber.
- The longitudinal Young's modulus of a unidirectional lamina for a typical glass fiber/epoxy composite showed a linear relationship with increasing the fiber volume fraction; nevertheless, the S-glass showed a little higher longitudinal Young's modulus than that of the E-glass composite.
- As the glass fiber volume fraction increased, the transverse Young's modulus of the glass-epoxy composite lamina also increased up to 23.80 and 25 GPa respectively for E-glass and S-glass fibers when the fiber volume fraction was 0.9.
- The in-plane shear modulus of a typical glass fiber/epoxy lamina increased gradually up to 8.932 and 9.528 GPa for E-glass and S-glass respectively when the fiber volume fraction was 0.9.
- With an increasing fiber volume fraction, both the longitudinal and transverse coefficient of thermal expansion decreased gradually and reached the value 5.34 and 5.26, respectively; 12.51 and 12.49 for E-glass and S-glass lamina respectively when the fiber volume fraction was 0.9.
- The values obtained for the intended mechanical properties of typical glass fiber/epoxy lamina by means of the Halpin-Tsai equation in comparison to experimental data and the strength of materials approach data are the most suitable for industrial applications.

The analytical results of micro mechanics were again compared with the results of a case study from micro to macro-mechanical analysis. The case study results, and their comparison show:

- After certain instances with increasing volume fraction of glass fiber the Young's Modulus of the composites decreased.
- Due to increasing the number of laminas, inadequate adhesion at the interfacial level and voids between the fibers and particles, the micro-mechanical analysis results did not correspond to the macro-mechanical analysis results.

Acknowledgements

Atomic Energy Commission, Savar Institute of Radiation and Polymer Technology Energy Laboratory, Dhaka University of Engineering and Technology Military Institute of Science and Technology, Mirpur

REFERENCES

- [1] Paresh K., Charmis D., Micromechanics analysis of fiber reinforced composite, *International Journal of Engineering Research and Technology* 2015, 4, 05, 439-446.
- [2] Koley S., Mohite P.M. Upadhyay C.S., A micromechanical study and uncertainty quantification for effective properties of unidirectional fibre reinforced composites, *Composite Structures*, 2019, 225(111141).
- [3] Yang Y., Micromechanics - based analyses of short fiber-reinforced composites with functionally graded interphases, *Journal of Composite Materials* 2019, 0, 0, 1-18.
- [4] Mozafari H., Dong P., Ren K., Han X., Gu L., Micromechanical analysis of bioresorbable PLLA/Mg composites coated with MgO: Effects of particle weight fraction, particle/matrix interface bonding strength and interphase, *Composites Part B: Engineering* 2018, 162, 129-133.
- [5] Erden S., Enhancement of the mechanical properties of glass/polyester composites via matrix modification glass/polyester composite siloxane matrix modification, *Fibers and Polymers* 2010, 11, 5, 732-737.
- [6] Li S., Boundary Conditions for unit cells from periodic microstructures and their implications, *Composites Science and Technology* 2008, 68, 1962-1974.
- [7] Krishna Golla S., Prasanthi P., Micromechanical analysis of a hybrid composite-effect of boron carbide particles on the elastic properties of basalt fiber reinforced polymer composite, *Materials Research Express* 2016, 3, 11, 115303.
- [8] Daggumati S., Sharma A., Pydi Y.S., Micromechanical analysis of FE analysis of SiCf/SiC composite with BN interface, *Silicon* 2020, 12, 2, 245-261.
- [9] Pyrz R., *Micromechanics of Composites*, Department of Mechanical Engineering, Alborg University 2008.
- [10] Zheng-Ming Huang, On micromechanics approach to stiffness and strength of unidirectional composites, *Journal of Reinforced Plastics & Composites* 2018, 38, 4, 167-196.
- [11] Hashin J., *Analysis of composite materials*, ASME, J. Appl. Mech. 1983, 50, 481-505.
- [12] Judd N.C.W., Wright W.W., Voids and their effects on the mechanical properties of composites - an appraisal, *SAMPE J.*, 1978, 10-11.

- [13] Raffi M., Ramgopal Reddy B., Effect of epoxy modifiers (bagasse fiber/bagasse ash/ coal powder/ coal fly ash) on mechanical properties of epoxy/glass fiber hybrid composites, *International Journal of Applied Engineering Research (IJAER)* 2015, 10, 24, 45625-45630.
- [14] Li L., Aliabadi F., Wen P.H., Micromechanical continuum damage analysis of plain-woven composites', *Journal of Multiscale Modelling* 2016, 6, 3, 1550009 (34 pages).
- [15] Hasanzadeh-Aghdam M.K., Ansari R., Mahmoodi M.J., Micromechanical analysis of the elastic response of glass-epoxy hybrid composites containing silica nanoparticles, *Mechanics of Advanced Materials and Structures* 2018, 26, 23, 1920-1934.